Vol. 519: 75–87, 2015
doi: 10.3354/meps11097

MARINE ECOLOGY PROGRESS SERIES
Mar Ecol Prog Ser

Published January 20

Interannual variations in phytoplankton community structure in the northern California Current during the upwelling seasons of 2001–2010

Xiuning Du[1,*], William Peterson[2], Linda O'Higgins[1]

[1]Cooperative Institute for Marine Resources Studies, Oregon State University, Newport, Oregon 97365, USA
[2]National Oceanographic and Atmospheric Administration–Fisheries, Hatfield Marine Science Center, Newport, Oregon 97365, USA

ABSTRACT: Phytoplankton species were enumerated from 72 samples collected biweekly during the upwelling season (May to August) of 2001–2010 to test for effects of interannual variations in upwelling and decadal basin-scale variability on phytoplankton species composition and community structure. Cluster analysis of phytoplankton community structure identified 7 groups; 1 group was dominated by dinoflagellates while the other groups were dominated by diatoms but with variable ratios of diatom-to-dinoflagellate abundance ranging from 4 to 847. The most abundant diatoms were *Thalassiosira* spp., *Chaetoceros* spp., *Asterionellopsis glacialis*, *Cylindrotheca closterium*, *Leptocylindrus* spp., *Nitzschia* and *Pseudo-nitzschia* spp., with dominance varying among the 7 groups. Variations in phytoplankton community structure were not related to the strength of upwelling within a given year; rather, differences were related to when a sample was collected within an upwelling/downwelling cycle. Community structure was also analyzed by non-metric multidimensional scaling ordination. The *x*-axis scores of the ordination, which is an index of community structure, were correlated with the Pacific Decadal Oscillation (PDO) but not with seasonally averaged coastal upwelling strength. Positive values of the index corresponded with positive PDO years (2002–2007), and negative index values with negative PDO years (2001, 2008–2010). Thus changes in the sign of the PDO seem to be more influential in explaining the interannual variations in phytoplankton community structure than seasonally averaged coastal upwelling.

KEY WORDS: Diatom · Dinoflagellate · Northern California Current · Coastal upwelling · Pacific Decadal Oscillation

INTRODUCTION

Variability in phytoplankton biomass in the California Current system has been well-described in terms of satellite-derived ocean color data at multiple time (from season to decade) and spatial scales. A wealth of satellite images illustrate responses of phytoplankton to coastal upwelling (Yoo et al. 2008, Thomas et al. 2009, Tweddle et al. 2010, Thomas et al. 2012), phase shifts of the El Niño Southern Oscillation (ENSO), the Pacific Decadal Oscillation (PDO) (Henson & Thomas 2007, Martinez et al. 2009), and to effects of wind-intensification at prominent capes and headlands (e.g. Checkley & Barth 2009). While ocean color images have provided good insights into the causes of temporal and spatial variations in the biomass of phytoplankton, such analyses yield few mechanistic insights into phytoplankton population dynamics at the species level in relation to environmental forcing because phytoplankton blooms are seldom monocultures. Siegel et al. (2013) provide an assessment of the utility of satellite chlorophyll prod-

*Corresponding author: xiuningdu@gmail.com

ucts as well as their limitations as a proxy for phytoplankton biomass (due to changes in chlorophyll per cell as a response to light) and species composition.

Ship-based collections provide the core information on phytoplankton species composition and community structure throughout the California Current. Available information on the larger phytoplankton species shows that diatoms contribute the most to total phytoplankton biomass, with the common and dominant taxa including *Chaetoceros*, *Thalassiosira*, *Pseudo-nitzschia*, *Asterionellopsis*, *Skeletonema*, *Leptocylindrus* and *Nitzschia* (Lassiter et al. 2006, Frame & Lessard 2009, Venrick 2012). These same genera dominated the diatom assemblage sampled in the southern California Current from 1920–1939 (Tont 1987) and from 1954–1960 (Bolin & Abbott 1963). Seasonality of phytoplankton is strong, with the highest abundance during the spring and summer and lowest during the winter in the southern (Venrick 2012), central (Garrison 1979) and northern parts of the California Current (Du & Peterson 2014). Relative abundances of the dominant species are not always the same within a season/year and are sensitive to changes within active/relaxed upwelling events (Frame & Lessard 2009, Du & Peterson 2014).

A limited number of studies have focused on the interannual variations in phytoplankton species in the California Current system. One of these studies, in the California Cooperative Oceanic Fisheries Investigation (CalCOFI) region off southern California by Venrick (2012), found that there was a long-term trend towards an increase in phytoplankton biomass over the time period of 1990–2009 (albeit a decline in the warm EI Niño years). She also reported a shift in the timing of the annual peaks of phytoplankton biomass in 1998, from spring to summer, as well as a change in species composition (a 75% decrease in the diatom *Hyalochaete*). In Monterey Bay (central California Current), there was evidence for a shift from a diatom-dominated community to a dinoflagellate type in summer 2004, shown by a notable decrease in the diatom *Pseudo-nitzschia* but significant increases in the toxic dinoflagellates *Alexandrium* and *Dinophysis* (Jester et al. 2009). A study off Bodega Bay (central California; Lassiter et al. 2006) reported that during the upwelling seasons of 2000–2002, the phytoplankton community was dominated by the diatoms *Chaetoceros*, *Asterionella*, *Thalassiosira*, *Guinardia* and *Nitzschia* (Lassiter et al. 2006). A similar study on the Washington coast in 2004–2006 (Frame & Lessard 2009) reported *Thalassiosira* dominated in summer 2004 and spring 2006 and *Chaetoceros* in summer 2005.

During the decade of 2001–2010, strong seasonal and interannual variability in upwelling and large-scale climate forcing was observed throughout the California Current, with alterations between years of strong and weak upwelling, positive (warm) and negative (cool) phases of the PDO, as well as the occurrence of several El Niño events (Peterson & Schwing 2003, Checkley & Barth 2009). In the northern California Current, subtropical zooplankton dominate during periods of the weak-upwelling, positive phases of the PDO and El Niño events, but subarctic zooplankton dominate during strong-upwelling, negative phases of the PDO and La Niña events (Peterson et al. 2002, Peterson 2009, Keister et al. 2011, Francis et al. 2012). Ichthyoplankton respond in a similar fashion (Auth et al. 2011). Given the pronounced signals in copepods and fish larvae, do phytoplankton species respond in a similar manner? In this study, 2 main questions were investigated. Firstly, were the observed patterns in phytoplankton abundance, species composition and community structure driven by interannual variations in local upwelling or by large-scale climate forcing such as PDO? Secondly, during the upwelling season, could temporal variability in phytoplankton community structure be attributed to the strength of the upwelling or to when the samples were collected during the upwelling/relaxation event cycles? These questions were examined using a 10 yr time series of phytoplankton data collected biweekly from May through August in the Oregon upwelling zone, months that represent the period of most active upwelling. High-frequency sampling was used as this method helps to capture variability in community structure associated with upwelling events, whereas sampling over a decade provides information on variability associated with the PDO.

MATERIALS AND METHODS

Data sources

Phytoplankton and hydrographic data were collected biweekly during the upwelling season from May to August 2001–2010. Data were collected from a station (Stn NH5; Fig. 1) located 9 km from shore, in 62 m of water along the Newport Hydrographic Line (44.6° N, 124.2° W) off central Oregon, USA. On each cruise, surface water samples were collected for the analyses of phytoplankton species, chlorophyll *a* (chl *a*) and nutrients (nitrate, NO_3; silicate, SiO_4; phosphate, PO_4). Chl *a* subsamples (each of 100 ml) were

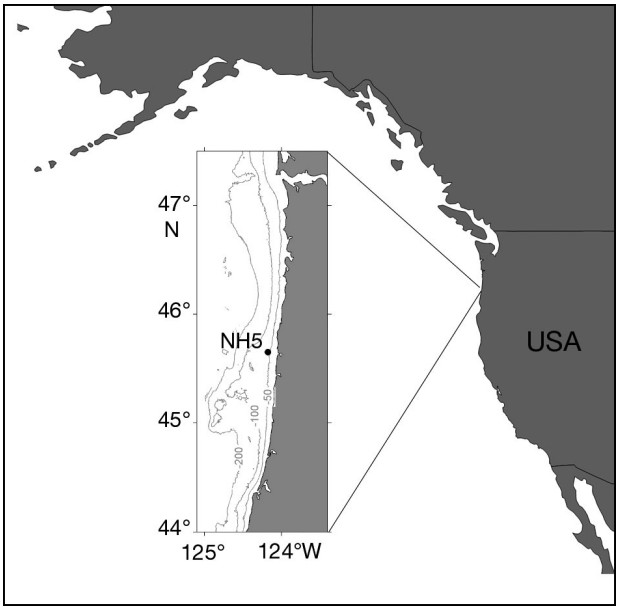

Fig. 1. Location of sampling Stn NH5 (44.6° N, 124.2° W) off central Oregon, USA in the Pacific Northwest

filtered through GF/F filters, extracted in 90% acetone for 24 h in the dark, and then fluorescence was measured using a Turner 10-AU fluorometer. The concentration of chl *a* was calculated following equations in Strickland & Parsons (1972). Nutrients were processed using a Technicon Autoanalyzer, following standard protocols. Vertical profiles of temperature and salinity were collected with a Seabird SBE 19 CTD.

A total of 72 phytoplankton samples were collected, and each was fixed with formalin (final concentration 2%) in 150 ml bottles. To enumerate species, a subsample of 50 ml was taken from the full sample and then settled in a 50 ml tissue culture flask (Falcon) for at least 24 h prior to counting. The wide flat side of the flask was placed on the stage of an inverted light microscope (Leica DM IRB); species identification and enumeration were carried out at magnifications of 200× or 400×. Nanoflagellates were not enumerated since diatoms and dinoflagellates were the focus of this study. The portion of the 50 ml subsample that was examined varied with species density. To meet a minimum count of 500 cells, between 2 and 20 transects across the wide side of the flask were counted; the whole subsample was necessarily checked for less common species. The total cell abundance of diatoms and dinoflagellates was calculated as numbers per liter (cells l^{-1}). Species identification was made primarily following Horner (2002).

Preservation with formalin can create problems in identifying the smaller naked dinoflagellates to species or genus level. Given this problem, those species were pooled into one group called 'small dinoflagellates'. Formalin preservation can also cause inacurracies in the calculation of cell volume; however, our focus in this study was changes in species and abundance, not cell volume or carbon. Diatoms were the dominant group throughout the upwelling seasons, and therefore had much higher weight in determining the patterns of phytoplankton community structure.

The Upwelling Index (UI, a measure of the volume of water upwelling, in units of $m^3\ s^{-1}$ per 100 m coastline), obtained from www.pfeg.noaa.gov for data at latitude 45° N, was used to indicate upwelling strength at the study site. A cumulative UI (CUI) was calculated by sequentially adding the daily UI values from May to August. Upwelling was also characterized by water temperatures in the upper 20 m of the water column. Monthly temperature anomalies were calculated by subtracting monthly temperatures in each year (2001–2010) from the long-term monthly averaged temperatures, using all data from 1997–2013. Daily wind stress observed at Newport (http://damp.coas.oregonstate.edu/windstress/index.html) was used to define upwelling and relaxation events.

Because there can be a succession of the phytoplankton species composition within the cycle of upwelling/relaxation events, each sampling date was classified by the number of days that either upwelling or relaxation had occurred before the sample was collected. For samples collected during upwelling events (mostly 2 to 28 d with an average of 10.4 d), 'the number of days' was standardized as to the ratio of the 'days into an event' divided by the 'total days' of the event. A ratio close to 0 indicates a sampling date that was early in the evolution of an upwelling event, and close to 1 indicates near the end of an upwelling event. Accordingly, total dates (n = 50) sampled during upwelling events were divided into 6 groups (a to f), where a = 1 to 2 d into the event; for samples collected ≥3 d after the beginning of an event, b: ratios < 0.4; c: 0.4 ≤ ratios < 0.6; d: 0.6 ≤ ratios < 0.8; e: 0.8 ≤ ratios < 1; and f: ratio = 1. All samples collected during the relaxation events (n = 22) were divided into 2 groups (g to h) based on the days of relaxation before sampling: g = Days 1–2; h = Days 3–5 plus 2 dates sampled 8 and 11 d after relaxation. Eighteen out of these 22 relaxation samplings had a duration of ≤5 d. This analysis was then used to produce a climatological picture of the response of sea surface temperature (SST), nutrients and phytoplankton during a typical cycle of upwelling/relaxation.

The PDO is a climate index based upon spatial patterns of variation in SST of the North Pacific (Mantua & Hare 2002). The PDO has 2 phases: a warm phase (positive values of PDO) generally corresponding with anomalously warm California Current, and a cold phase (negative PDO) corresponding to cold California Current. In contrast to the local SST variations directly associated with upwelling, the PDO index of SST variation indicates changes in ocean conditions at a basin scale. Monthly values of the PDO are available at http://jisao.washington.edu/pdo, thus can only be used to examine relationships between phytoplankton species composition on a monthly–seasonal basis.

Community structure analysis

Differences in the phytoplankton community structure among the 72 sampling dates were examined using hierarchical cluster analysis (CLUSTER) and non-metric multidimensional scaling (NMDS) on a Bray-Curtis similarity matrix. Only species with an occurrence rate >5% in the 72 samples were included. All data were log(x + 1) transformed to reduce the influence of extremely abundant species. Similarity of profile (SIMPROF) determined significant differences among phytoplankton clusters SIMPER determined the percent contribution of different species to the significant clusters. From the 2-dimensional (x-, y-axis) NMDS results, the x-axis scores were defined to be the 'phytoplankton community structure' index. Both 1-way and 2-way ANOSIM were used to test for differences in the phytoplankton community across the different factors—years, PDO phases and upwelling states. The statistic R (scaled to a range of values from 0 to 1) in ANOSIM is a measure of community separation between groups, with 0 indicating no separation and 1 indicating complete separation. Principal component analysis (PCA) examined patterns in the environmental variables (temperature, salinity and nutrients) across sampling dates. All environmental data were normalized and the PCA was run on a Euclidean distance matrix. The relationship between environmental variables and phytoplankton communities was examined by BEST/BIO-EVN. The environmental variables (individual or combinations) with the highest Spearman's rank correlation coefficient (ρ) suggest which variables best explain the patterns in the phytoplankton community. All the above multivariate analyses were conducted using PRIMER-E software (Clarke & Gorley 2006).

RESULTS

Interannual fluctuations in upwelling and temperature

The intensity of upwelling is depicted in the slope of the CUI lines—strongly positive slopes indicate a more intensive upwelling (Fig. 2A). Obvious decreases in the slope of the CUI line and brief changes from positive to negative indicate weak upwelling or relaxation of upwelling. Over the May to August period, much stronger upwelling (CUI > 6000 units) was observed in 2003 and 2006, followed by CUI = 5500 in 2001–2002, and values of 4000 to 5000 in 2008 and 2010. Low upwelling intensity (3500 to 4000) was observed in the years 2004, 2005, 2007, and 2009.

SST anomalies at Stn NH5 (Fig. 2B) were 1.2°C above average in both 2004 and 2005, close to the average in 2007, but colder than the average for all other years, especially 2002 (–1.0°C), 2008 (–0.75°C) and 2009 (–0.66°C). SST did not correlate with seasonally-averaged upwelling strength (r = –0.3, p = 0.35). Even though the warm years 2004 and 2005 corresponded with lower CUI values (warm SST and weak upwelling), the coldest year (2002; –1.0°C) had only moderate upwelling, and years with the maximum CUI (2003 and 2006) only had temperature anomalies of –0.25 and –0.18°C, respectively. Some of the coldest anomalies were seen in 2008 and 2009 when the CUIs were well below the average (CUI = 4813). In contrast, the SST was correlated with the PDO (r = 0.66, p = 0.04), illustrating that basin-scale processes may have a greater influence on SST than local upwelling.

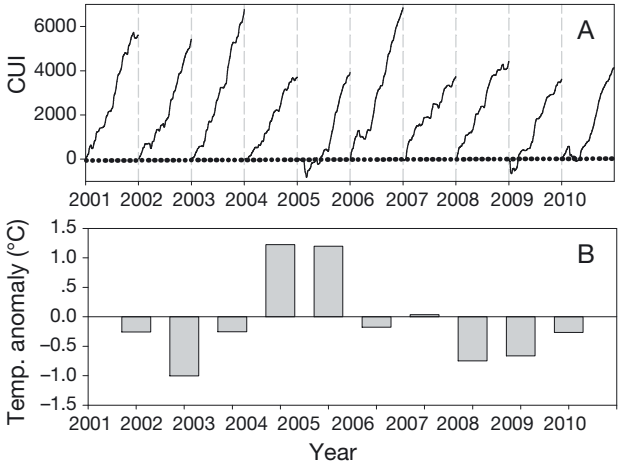

Fig. 2. (A) Total amount of upwelled water (cumulative upwelling index, CUI, m^3 s^{-1} per 100 m of coastline) from May to August of 2001–2010, and (B) temperature anomalies at Stn NH5 at an average of 20 m depth

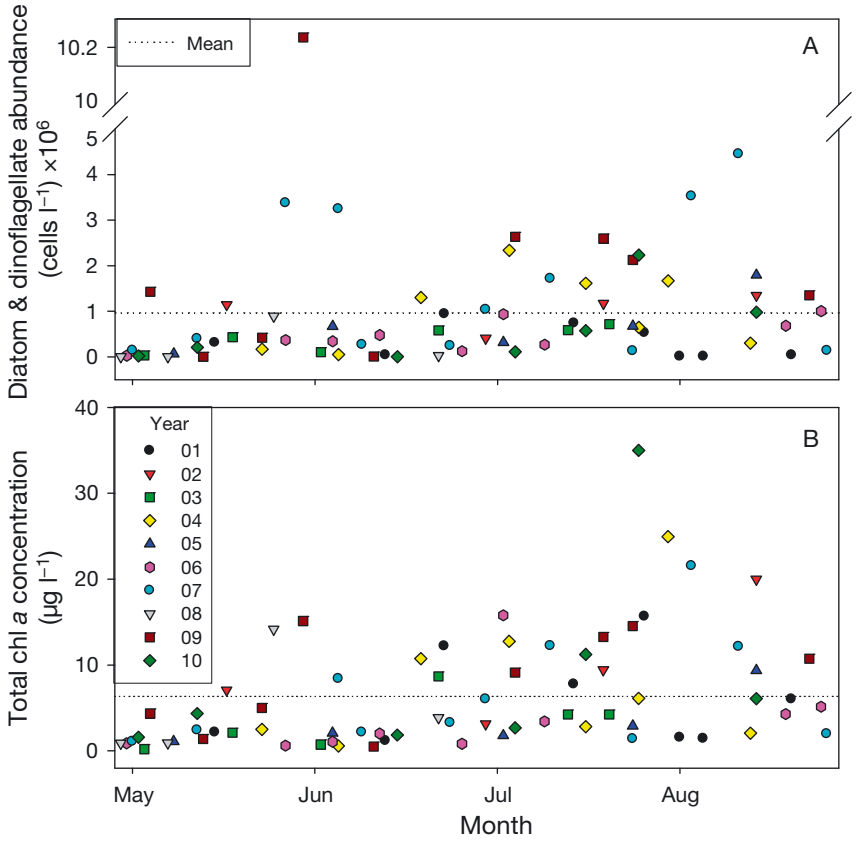

Fig. 3. (A) Climatological variations in cell abundance of diatoms and dinoflagellates and (B) total chl *a* concentration from May to August of 2001–2010 (sample numbers: n = 72)

Interannual variability in phytoplankton community

Abundance. The average total abundance of diatoms and dinoflagellates combined during May to August (2001–2010) was 963 588 cells l^{-1} (Fig. 3A, n = 72, range of 560 to ~10 235 276 cells l^{-1}); 22 samplings (31% of total) had an abundance >1 000 000 cells l^{-1}. Most of the high abundances appeared in July (9 records) and August (7 records), and less often in May and June (3 records each). There was a weakly positive trend in abundance with year (r = 0.22, p = 0.07).

Chl *a*. The mean concentration of chl *a* was 6.3 µg l^{-1} (n = 72, range of 0.2 to ~35 µg l^{-1}). There were 24 observations (33% of all) above the mean. Most of the high values were found in July (11 records) and August (6 records) followed by June (5 records) and May (2 records). Total chl *a* (Fig. 3B) was linearly correlated with cell abundance (r = 0.55, p < 0.0001), however, there was no significant trend in changes of chl *a* concentration with year (r = 0.1, p = 0.39).

Community structure. Phytoplankton community structure showed significant differences among years (1-way ANOSIM, R = 0.33, p < 0.001). Cluster analysis produced 7 groups (Table 1) that were significantly different (p < 0.01, 45% resemblance level); the spatial orientation of these 7 groups, labeled as G1 to G7 in the polygons, along with 3 single 'outlier' sampling dates are shown in the NMDS plot (Fig. 4). The 7 groups were sorted by a 'northeast–southwest' directed diagonal line. To the left of this line are groups with relatively low abundance and to the right, groups with higher abundance.

G1 was the only group dominated by dinoflagellates and included sampling dates only from the year 2007 (Table 1). The other groups were all

Table 1. Phytoplankton community groups (G1 to G7) identified from cluster analysis. For each group, sampling dates, diatom and dinoflagellate combined abundance (diat+dino) and ratios between them (diat:dino) are shown

Groups, year (dates; mm/dd)	Abundance diat+dino (cells l^{-1})	Ratio diat:dino
G1 2007 (6/27, 7/3, 7/28)	467 595	0.1
G2 2001 (5/18, 6/16, 6/26, 7/18, 7/30); 2010 (7/8)	442 533	13.7
G3 2006 (5/3); 2007 (8/7, 8/15, 8/30)	2 028 368	408.8
G4 2002 (7/23, 8/18); 2009 (5/7, 5/26, 6/2, 7/8, 7/23, 7/28); 2010 (7/20, 7/29, 8/18)	2 330 813	846.6
G5 2002 (5/20, 7/3); 2003 (5/6, 5/21, 6/5, 6/25, 7/17, 7/24); 2004 (5/25, 6/7, 6/21, 7/6, 7/19, 7/28, 8/2, 8/17); 2005 (5/11, 6/7, 7/6, 7/28, 8/18); 2006 (5/30, 6/15, 6/7, 6/29, 7/6, 7/13, 8/23, 8/29); 2007 (5/15, 5/30, 6/8, 6/12, 7/14); 2009 (8/27); 2010 (5/15)	840 656	35.5
G6 2001 (8/9); 2008 (5/9, 6/24); 2010 (5/5, 6/18)	8998	4.1
G7 2001 (8/5, 8/24), 2008 (5/1, 5/27)	231 411	18.6

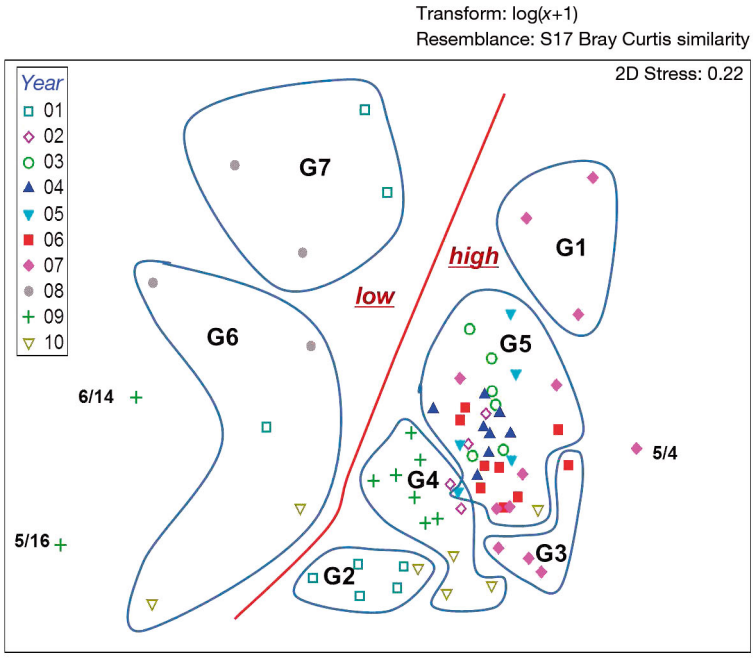

Fig. 4. Non-metric multidimensional scaling analysis of diatom and dinoflagellate community patterns from May to August of 2001–2010. Each of the G1 to G7 groups is enclosed by the blue lines. The diagonal red line divides the groups by 'low' and 'high' abundance of diatoms and dinoflagellates combined. Three single and ungrouped 'outlier' dates (mm/dd/yy) are indicated: 5/4/07, 5/16/09 and 6/14/09

diatom-dominated but with diatom-to-dinoflagellate ratios ranging from 4 to 847; G5 had a medium to high average abundance and included samples from all of 2003–2005, plus a few from other years. G4 showed the highest average abundance (2 330 813 cells l^{-1}) and diatom-to-dinoflagellate ratio (846.6); G3 followed G4 closely in both values. G2 had a relatively low abundance and low diatom-to-dinoflagellate ratio. The lowest average abundance groups were G6 (8998 cells l^{-1}) and G7 (231 411 cells l^{-1}). Two of the 3 'outlier' sampling dates, 5/16/2009 and 6/14/2009 (mm/dd/yyyy), had very low abundances of 560 and 6840 cells l^{-1}, respectively. The sample from 5/4/2007 was a diatom-dominated sample with slightly higher abundance (136 068 cells l^{-1}), but was an outlier because it lacked one of the dominant taxa (*Thalassiosira* spp.) commonly found in G2 to G5.

Species. Six of the 7 groups were dominated by diatoms. *Thalassiosira* spp. was dominant in G2 and G5 to G7, but *Chaetoceros* spp. dominated in G3 and G4 (Table 2). The sub-dominants included *Cylindrotheca closterium*, *Nitzschia* spp., *Asterionellopsis glacialis*, *Guinardia delicatula*, *Leptocylindrus danicus*, *Lauderia annulata*, *Pseudo-nitzschia* spp. and *Thalassionema nitzschioides*. The dinoflagellate group G1 was dominated by *Gymnodinium* spp., *Prorocentrum gracile* and *Scrippsiella trochoidea*.

Patterns by environmental variables

PCA reduced the 5 environmental variables (SST, sea surface salinity [SSS], PO_4, NO_3 and SiO_4) to 2 components (Fig. 5). PC1 explained 75.6% of the variations in the original variables and PC2 explained 16.1%. Four variables (PO_4, NO_3, SiO_4 and SST) contributed evenly to PC1 as shown by their coefficients in the linear regression of PC1: –0.503, –0.488, –0.429 and 0.425, respectively. SSS was the only primary variable with a high coefficient (0.729) that contributed to PC2.

The patterns of the environmental variables across the sampling dates depicted by PCA fell into 2 large groups, repre-

Table 2. Phytoplankton species or genus with % contributions to each of the CLUSTER groups are listed from SIMPER analysis. The 'cut-off' line for the listed taxa is when the cumulative percent contribution reached 50% in each group

	G1	G2	G3	G4	G5	G6	G7
Diatom							
Asterionellopsis glacialis		6.2	10.6				
Chaetoceros spp.		7.2	13.6	13.9	11.2		
Cylindrotheca closterium			11.2	7.7	9.0		
Guinardia delicatula		6.7					
Lauderia annulata		6.4					
Leptocylindrus danicus					7.5		
Nitzschia spp.			11.4	7.5	9.1		
Pseudo-nitzschia deli/p-deli					6.8		
Pseudo-nitzschia fraud/aust				9.1			
Pseudo-nitzschia multi/pung		5.6					
Thalassionema nitzschioides						22.8	
Thalassiosira rotula		8.5					
Thalassiosira spp.		10.2	12.8	11.7	11.7	25.9	39.2
Dinoflagellate							
Gymnodinium spp.	19.3						
Prorocentrum gracile	21.9						
Scrippsiella trochoidea	19.2						22.5

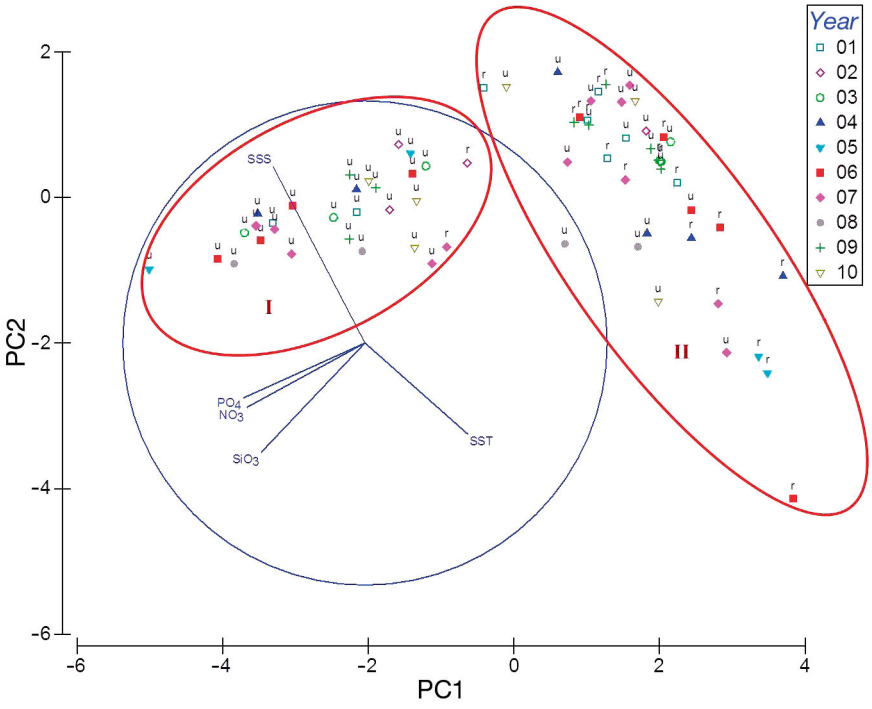

Fig. 5. Principal component analysis of the interannual patterns of upwelling related to environmental variables (SST, sea surface temperature; SSS, sea surface salinity; NO_3, nitrate; SiO_4, silicate; PO_4, phosphate). The symbols indicate sampling dates in different years. The lowercase letters corresponding with symbols indicate upwelling (u) or relaxation (r) when samplings were occurring. Two groups (I and II) were separated in the ellipses. Group I is an active upwelling group; Group II is a relaxed upwelling group

senting the state of upwelling (active vs. weak/relaxed). One group (I) was comprised mostly of sampling dates with active upwelling (n = 28 of 72 dates) while the second group (II) was related to both weak upwelling and relaxation (n = 44 of 72 dates). Group I was characterized by higher nutrients (e.g. average NO_3: 18.5 ± 5.7 µM) and lower temperatures (average 9.7 ± 1.2°C), while Group II had lower nutrients (NO_3: 1.8 ± 4.7 µM) and higher temperatures (average 12.5 ± 2.0°C).

Relationships between phytoplankton community structure and environmental forcing

Connections with upwelling. Correlations between phytoplankton community structure and upwelling were tested in several ways. Firstly, the correlation between the phytoplankton community matrix and environmental variable matrix (tested by BEST) was weak, with the highest Spearman rank coefficient, ρ, only 0.123, indicating neither individual nor combinations of the environmental variables (nutrients, temperature and salinity) was well associated with phytoplankton community structures. Secondly, the linear correlation between CUI and the community structure index (the *x*-axis score from NMDS) was not significant (r = 0.2, p = 0.6). Thirdly, the 2-way crossed ANOSIM showed the variance in phytoplankton community structure explained by states of upwelling (active, weak or relaxed) across years was not significant (R = 0.069, p = 0.27) while there was higher variance explanation by 'year' (R = 0.399, p < 0.001). Fourthly, correlation between the seasonally-averaged CUI and seasonally-averaged phytoplankton cell abundance was not significant (r = 0.56, p = 0.1).

The environmental differences across the states of upwelling/relaxation (periods a through h; ANOSIM, R = 0.201, p < 0.001) were clearly seen from the temperature vs. nitrate plot, which illustrates the general evolution of the physical and chemical conditions during an upwelling/relaxation cycle (Fig. 6A). One to 2 d after the beginning of the upwelling events (a in Fig. 6A), the temperature was cool (11.7°C) and nitrate level was 5 µM; after the third day of upwelling (b, c, and d in Fig. 6A), the temperature had dropped to 10°C and nitrate had increased to 15–20 µM; e and f reflected conditions near the end of an active upwelling event whereas g and h characterized relaxation of upwelling when the waters warmed and nutrients were depleted (13°C and <2 µM nitrate; Fig. 6A).

There were corresponding changes in phytoplankton during the same upwelling/relaxation cycle (Fig. 6B, Table 3). During the very early stage of upwelling events (a), concentrations of both chl *a* and nitrate were low. During the midpoint of upwelling events (b→e), abundance and chl *a* increased from a low concentration (b) to a medium-high level (c→d→e); nitrate reached a maximum (b→c→d) but then decreased (e). Near the end of upwelling events (f), the highest abundance and chl *a* concentrations were observed as well as increased temperature but decreased nitrate concentration. Early relaxation events (g) were characterized by continued higher abundance and chl *a* but still decreasing nitrate; near the

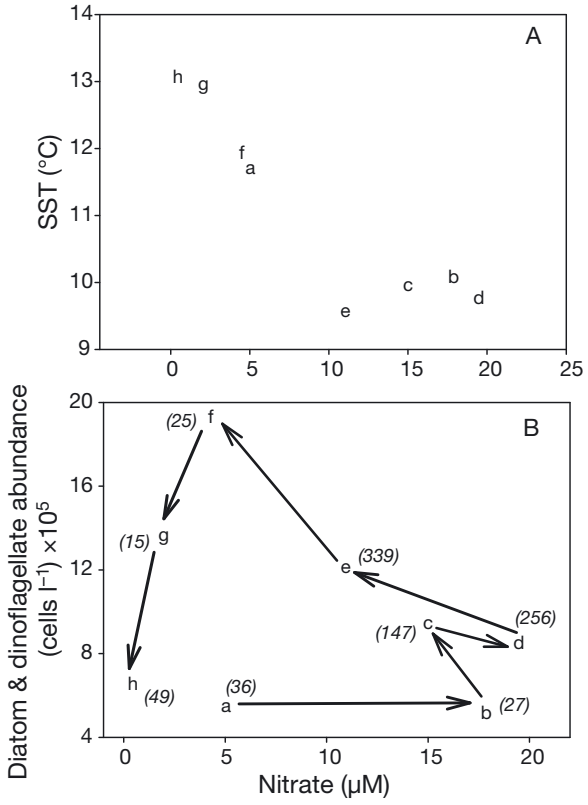

Fig. 6. (A) Climatological relationships between nitrate concentration and sea surface temperature (SST). (B) Diatom and dinoflagellate abundance combined versus nitrate concentration. Letters a through h stand for different states of upwelling process, with a and b being early in the upwelling event, c, d and e the middle of an upwelling event, f the end of an active upwelling event, and g and h the relaxation of upwelling. The numbers in italics are the ratios of diatoms-to-dinoflagellates (as in Table 1) for the corresponding groups, a through h

very end of relaxation events (h), abundance and chl *a* declined to the level similar to a, accompanied with the highest temperature and the lowest nitrate levels. The ratios of diatoms to dinoflagellates were low at the beginning of upwelling events (36 and 27 during a and b, respectively) and highest (147→339) during the upwelling periods of c→d→e, corresponding with diatom blooms. Reduced ratios during f (25) and g (15) periods indicate a relatively greater contribution from dinoflagellates to the community at the end of active upwelling events.

Changes in total phytoplankton abundance were rapid, ranging from ~500 000 cells l^{-1} on average during upwelling periods a and b, with a doubling during periods c and d, and another doubling during e→g. Numbers collapsed to ~650 000 cell l^{-1} during relaxation period h, resembling periods a and b.

Changes in the taxonomic composition of diatoms and dinoflagellates were not as pronounced as for SST, nitrate, total chl *a* and cell abundance (Table 3). Numerically, diatoms were always the dominant taxa, with several species of *Chaetoceros* dominating all events except b; *Thalassiosira* spp. was the dominant taxa in b; the second ranked taxa were *Asterionellopsis glacialis* (c), *Thalassiosira* spp. (d, e and g) and *Leptocylindrus danicus* (f). Other dominant taxa included *Pseudo-nitzschia* spp. and *Nitzchia* spp. Dinoflagellates were the 5th or 6th most dominant taxa very early in an upwelling event (b), towards the end of an upwelling (f) and during relaxation (g and h). The dominant species at these times were usually *Scrippsiella trochoidea* (b and g) or *Gyrodinium spirale* (f and h).

Table 3. Average chl *a* concentration (µg l^{-1}), sea surface temperature (SST, °C), sea surface salinity (SSS), nitrate and silicate concentration (µM) and diatom and dinoflagellate abundance (diat+dino, cells l^{-1}), in the groups defined by states of upwelling and relaxation events. Also shown for reference are the average abundances (cells l^{-1}) for the dominant taxa in each group. Aster: *Asterionellopsis glacialis*; Chae: *Chaetoceros*; Cylin: *Cylindrotheca closterium*; Lept: *Leptocylindrus*; Nitz: *Nitzschia*; P-n: *Pseudo-nitzschia*; Thal: *Thalassiosira*

	Group (no. of samples)							
	a(16)	b(9)	c(5)	d(8)	e(6)	f(6)	g(15)	h(7)
Chl*a*	4.1	4.2	7.2	3.7	15.8	10.0	7.2	3.3
SST	11.7	10.1	10.0	9.8	9.6	11.9	13.0	13.1
SSS	31.9	33.1	33.1	33.3	33.3	32.4	31.4	32.0
Nitrate	5.0	17.8	15.0	19.5	11.0	4.5	2.0	0.4
Silicate	12.8	28.9	27.3	34.5	22.1	13.0	12.2	3.8
Diat+dino	551376	516646	945763	854490	1207901	1951730	1386538	655128
Dino	14711	18666	6397	3326	3553	75242	88935	13072
Aster	49207	43369	164266	99345	95443	139735	212187	35693
Chae	222560	79732	400405	351771	646031	877474	532728	382364
Cylin	12244	3130	7537	22103	9402	14476	75557	10207
Lept	81969	40703	44894	39519	49306	181708	118702	6719
Nitz	24429	7893	49995	26508	23394	24496	15888	18467
P-n	51178	33544	71848	38713	58861	152981	65101	35058
Thal	47700	82864	59879	201326	95287	142620	165034	30131

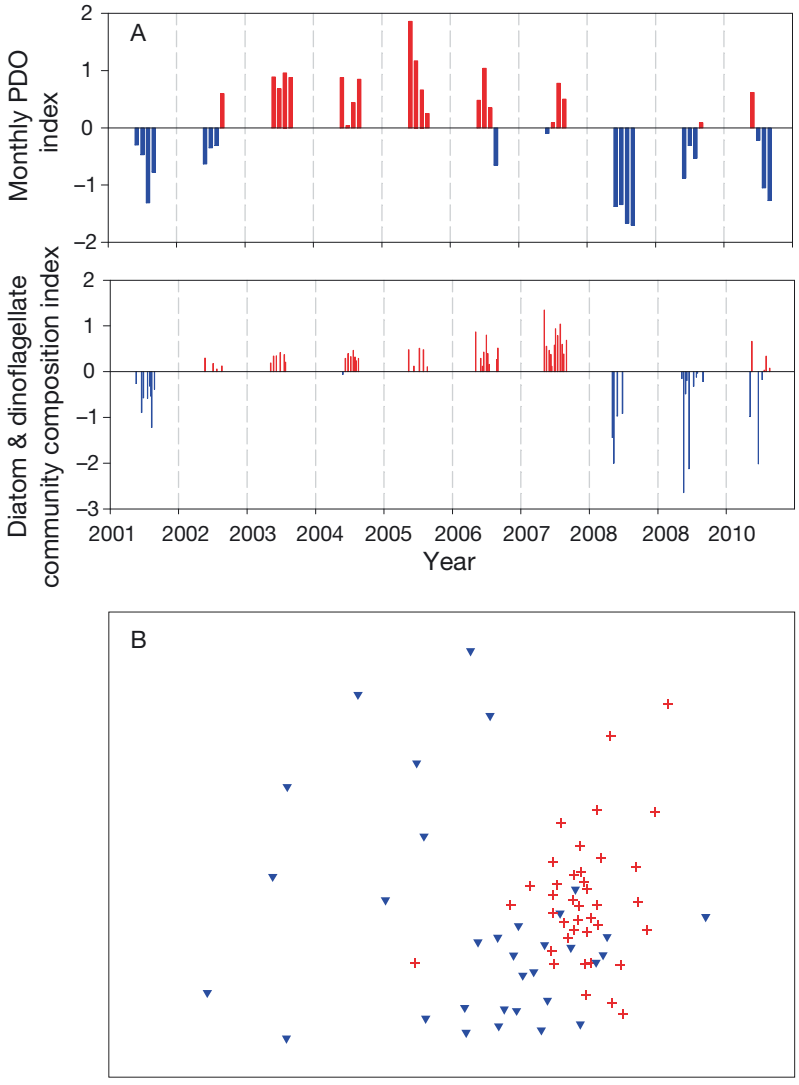

Fig. 7. (A) Patterns in the Pacific Decadal Oscillation (PDO) and the diatom and dinoflagellate community structure based on the monthly averaged *x*-axis scores from non-metric multidimensional scaling ordination (NMDS). (B) Spatial correlations between PDO phases (negative: blue inverted triangle; positive: red plus) and phytoplankton cluster groups shown in the NMDS plot

Connections with PDO. The phytoplankton community structure index (the monthly-averaged *x*-axis scores from NMDS) was correlated with the PDO (Fig. 7A; ANOSIM, R = 0.206, p < 0.001). There were 2 types of phytoplankton communities, one with a positive community index which included the years 2002–2007, and the other with mostly negative scores which included the years 2001 and 2008–2010. When the data shown in the NMDS plot (Fig. 4) are classified by the sign of the PDO on each sampling date (Fig. 7B), samples collected during the positive phase of the PDO were associated with CLUSTER groups G1, G3 and G5 whereas samples during the negative phase of the PDO were from groups G2, G4, G6 and G7 (several from G5).

Three diatom taxa were most abundant during the negative phase of the PDO: *Thalassiosira* spp., *Chaetoceros* spp., and *Asterionellopsis glacialis* (Table 4). The first 2 diatom taxa were also top-ranked during the positive phase of the PDO, along with *Cylindrotheca closterium*, *Leptocylindrus* spp. and *Pseudo-nitzschia* spp. Dinoflagellates had greater abundance during the positive phase of the PDO.

When the effects from PDO against upwelling were compared, the variation in phytoplankton community was explained much more by PDO (2-way crossed ANOSIM, R = 0.326, p = 0.001) than upwelling (R = 0.03, p = 0.256). Therefore, we conclude that the PDO is more influential than coastal upwelling in determining interannual variations in phytoplankton community structure.

DISCUSSION

The total abundance of diatoms and dinoflagellates combined and chl *a* concentration during our study were in the same range as for data reported elsewhere in the northern California Current. The range in chl *a* concentration off Newport (0.2 to 35 µg l^{-1}) was the same as the coastal upwelling systems off Bodega Bay (0.4 to 32 µg l^{-1}) (Lassiter et al. 2006) and off Washington (1 to 32 µg l^{-1}; Frame & Lessard 2009). Peak abundances in both the Lassiter study and ours were 4 to 9 × 10^6 cells l^{-1}. Further, 31% of our 72 samples had cell abundances >10^6 cells l^{-1}, which is remarkably similar to the 22 of 61 samples (or 36%) reported by Lassiter et al. (2006). Abundances in the southern California Current may be an order of magnitude lower, as Tont (1987) reported a maximum of 10^5 cells l^{-1} in winter, spring and summer, and 10^4 cells l^{-1} in autumn. Venrick (2012) reported the same magnitudes in cell abundance as Tont (1987) for the southern California Current.

There were no significant long-term trends in chl *a* concentration or in phytoplankton cell abundance

Table 4. Comparisons of average abundance (cells l^{-1}) of species (genus) and their ranks (based on their contribution to the similarity as a function of the phase of the PDO given by SIMPER analysis) along with individual percent contribution between groups under the negative (–) and positive (+) phase of the PDO. Aster: *Asterionellopsis glacialis*; Chae: *Chaetoceros*; Cos: *Coscinodiscus*; Cylin: *Cylindrotheca closterium*; Gyro: *Gyrodinium*; Lept: *Leptocylindrus*; Nitz: *Nitzschia*; P-deli: *Pseudo-nitzschia deli/p-deli*; P-multi: *Pseudo-nitzschia multi/pung*; P-fraud: *Pseudo-nitzschia fraud/aust*; Scrip: *Scrippsiella trochoidea*; Tnema: *Thalassionema nitzschioides*; Thal: *Thalassiosira*

Species	Av. abundance		Rank		Contribution%	
	(–)PDO	(+)PDO	(–)PDO	(+)PDO	(–)PDO	(+)PDO
Thal	135858	76863	1	1	17.5	11.5
Chae	542003	293206	2	2	12.2	11.0
Aster	171780	55861	3	8	7.9	5.7
Nitz	21200	22325	4	4	6.6	9.4
Cylin	7248	40242	5	3	4.8	10.7
Tnema	2011	6752	6	11	4.5	3.9
Cos	618	548	7	–	3.7	–
Lept	28807	96074	8	5	3.5	6.4
P-fraud	22384	25588	9	13	3.1	3.0
P-deli	18361	31178	10	7	3.0	5.8
P-multi	8041	12767	13	6	2.3	6.3
Scrip	425	4807	–	9	–	4.0
Gyro	307	3852	–	10	–	4.0

from this study. Venrick (2012), on the other hand, found an increase in chl *a* concentration between 1990 and 2010 as part of the CalCOFI program in the southern California Current, but no trends in phytoplankton abundance. A significant increase in chlorophyll (based on satellite-derived ocean color data) in the central California Current region over the time period 1996–2011 was reported by Kahru et al. (2012), but no long-term trend was observed in the northern California Current (Henson & Thomas 2007).

We did not find evidence to support the hypothesis that years of weak or strong upwelling accounted for the interannual differences in phytoplankton community structure. However, when our samplings were classified relative to the states of upwelling (Fig. 6, Table 3), phytoplankton abundance and the ratios of the 2 major functional groups (diatoms vs. dinoflagellates) followed the 'classical' physical–chemical patterns in the upwelling/relaxation cycles (e.g. Margalef 1978, Smayda & Reynolds 2001). Peaks in the abundance of diatoms occurred during the middle to the end of upwelling events as well as in the early relaxation period, whereas peaks in dinoflagellates occurred consistently during relaxation events and during the very early stages of upwelling events. Thus, our results conform to the well-known paradigm that dinoflagellates start 'blooming' near the end of upwelling events and continue into the relaxation period when nutrients and turbulence are low in the upwelling system, whereas diatoms start blooming during strong upwelling events when nutrients and turbulence are relatively high. These observations fit the classical pattern also described by Margalef (1978) and Smayda & Reynolds (2001). Smayda & Trainer (2010) discussed the diatom/dinoflagellate continuum in relation to the upwelling/relaxation cycles, and described a conceptual model similar to what we have presented (see their Fig. 2). Recently, Anabalon et al. (2014) reported a result similar to ours from a study of phytoplankton in the coastal upwelling region of the Canary Current. In their study, a different community (based on NMDS and cluster analysis) was found during 3 'states' of the upwelling process: moderate, weak and relaxation. Further, Pitcher et al. (1991) and Mitchell-Innes & Walker (1991) sampled daily for 28 d in shelf waters of the Benguela Current, and fortuitously sampled 2 complete upwelling/relaxation cycles. They showed that diatoms dominated early in an upwelling event, but during relaxation, diatoms diminished in biomass and the community changed gradually to a flagellate-dominated community.

Although a close temporal linkage at the scale of the upwelling/relaxation cycle existed between phytoplankton abundance and species composition, the correlation between upwelling strength averaged over an upwelling season (May through August) and either cell abundance or chl *a* concentration was not significant. Given that phytoplankton can draw down nutrients within a few days of the initiation of an active upwelling event (Wilkerson & Dugdale 1987), the cumulative phytoplankton production during the upwelling season should not be viewed as a function of the total amount of upwelling in a season, but rather as a result of the number, magnitude and duration of upwelling events within an upwelling season.

Another aspect of the problem of 'seasonal' vs. 'event-scale' upwelling is that wind speeds greater than a certain threshold may reduce productivity due to transport of phytoplankton offshore and out of the system; conversely, winds speeds less than the 'threshold' (or lack of equatorward winds) results in nutrients not being replenished frequently enough to reinvigorate phytoplankton blooms. One might ex-

pect to test the hypothesis of event-scale upwelling vs. total seasonal upwelling as drivers of seasonally integrated phytoplankton biomass using the extensive ocean color data sets, however, as Henson & Thomas (2007) pointed out, variability at the time scale of <10 d cannot be resolved due to cloud cover. Nutrient–phyto–zooplankton (NPZ)-upwelling modeling studies would be an appropriate way to investigate the optimal pattern of upwelling pulses by examining the response of phytoplankton and nutrients to the number of days of active upwelling vs. days of relaxation for a given region (as has been done by Yokomizo et al. 2010, for the central California Current region).

As for the correlation between phytoplankton community structure and the PDO, Henson & Thomas (2007) showed that the variance in ocean color in the California Current was correlated with the sign of PDO—the negative phase was associated with increased variance in the signal, and the positive phase with reduced variance. They suggested that this was due to variations in meso-scale eddy activity (e.g. weak in years with positive PDO).

We found differences in species abundance on average that were quite large for the first 3 dominant taxa between phases of the PDO (Table 4)—a factor of 2 to 3 lower abundance was observed when the PDO was positive compared to negative. Another difference was an order of magnitude increase in the abundance of the 2 dominant dinoflagellates, *Scrippsiella trochoidea* and *Gyrodinium spirale*, during the positive phase. Though species composition of the top 3 dominants were the same for the 2 phases, changes in the rank of some lower-ranked diatom species were observed: *Asterionellopsis glacialis* moved from rank 3 (negative PDO) to rank 8 (positive PDO) and *Thalassionema nitzschioides* from rank 6 to 11; *Pseudo-nitzschia deli/p-deli* and *Pseudo-nitzschia multi/pung* ranked higher during the positive phase of the PDO (rank 7 and 6 vs. 10 and 13, respectively). However, the question remains as to what might drive these differences. SST differences between the positive and negative phase of the PDO were at the most only ±1°C among years, but this might reflect subtle differences in water column stratification or possibly in growth rates of some species. The fact that dinoflagellates were an order of magnitude more abundant during the positive phase suggests perhaps changes in nutrients and stratification as a function of phase of the PDO. Differences in diatom dominance might be due to differences in the life history and physiology of the different species.

Another hypothesis that relates the PDO to plankton comes from studies of the copepods in the Oregon upwelling zone (Hooff & Peterson 2006). When the PDO is in negative phase, the copepod community found in the coastal waters off Oregon is dominated by lipid-rich copepod species which are common on the coasts of the Bering Sea and the Gulf of Alaska, whereas during the positive phase of the PDO, small warm-water subtropical species common to offshore Oregon and the coastal waters of the southern California Current become conspicuous. A hypothesis to account for this is that when the PDO is in negative phase, transport of waters from the coasts of the Gulf of Alaska into the northern California Current is strong, whereas during positive phases, transport within the California Current is weak, and more water moves onto the shelf from offshore during summer (Bi et al. 2011, Keister et al. 2011), or from the south in winter/spring with the Davidson Current. At this point, we do not know how variations in transport might affect phytoplankton community structure as opposed to the idea that seed stocks for blooms are maintained locally. Alternatively, zooplankton communities associated with changes of water masses (PDO phase related) might modify phytoplankton community structure through differential grazing behaviors, such as selective feeding.

Another alternate hypothesis is that the upwelling/relaxation cycles are a function of the phase of the PDO, and the optimal combination of days of upwelling and days of relaxation during an upwelling event are such that the negative (cool) phase of the PDO is a more productive period of phytoplankton than the positive (warm) phase. The best test would be done by daily sampling for at least 1 mo during several years with contrasting PDO phases. Modeling studies might be the most appropriate means of testing this hypothesis (e.g. Yokomizo et al. 2010 and Francis et al. 2012). However, when we compared the mean length of upwelling/relaxation events between years under negative and positive phases of the PDO, we found no differences in the duration (days) of both. For upwelling events during the negative phase of PDO (n = 23 dates), the average length of an event was 12.2 d, compared to the positive phase of PDO (n = 27 dates), with an average of 12.4 d. Similar results were obtained for relaxation events (negative phase of PDO: n = 10, average 3.5 d; positive phase of PDO: n = 12, average 3.8 d). Regardless, we find it curious that both phytoplankton and copepod community structure are better correlated with the basin-scale PDO than local coastal upwelling.

In conclusion, the main topic treated in this paper was the degree to which the observed patterns in community structure were related to variations in local upwelling vs. basin-scale variations associated with the PDO. The original hypothesis was that phytoplankton abundance and community structure would depend upon the strength of upwelling in a given year. However, we found no support for this hypothesis; rather, within-year variations in abundance and community structure were related with the event-scale of active/relaxed upwelling. Furthermore, among-year variations in community structure were significantly correlated with phase of the PDO.

Acknowledgements. We thank Leah Feinberg, C. Tracy Shaw, Rian Hooff, Jay Peterson, Jennifer Menkel, Jennifer Fisher, Karen Hunter and Bobby Ireland, who collected the samples over the years along the Newport Hydrographic Line that were analyzed in this study. Jennifer Fisher and Jay Peterson provided comments on earlier drafts of the manuscript. The manuscript also benefited from remarks by Dr. M. J. Dagg. Post-doctoral support for this study was provided to X.D. by a grant from the NOAA-MERHAB program, NA07NOS4780195. Support for L.O'H. was provided by a grant from the National Research Council (National Academy of Sciences) in 2006 and by the NOAA-MERHAB program, NA07NOS4780195 during the early phases of the program (2007 and 2008).

LITERATURE CITED

Anabalon V, Aristegui J, Morales CE, Andrade I and others (2014) The structure of planktonic communities under variable coastal upwelling conditions off Cape Ghir (31°N) in the Canary Current System (NW Africa). Prog Oceanogr 120:320–339

Auth TD, Brodeur RD, Soulen HL, Cianelli L, Peterson WT (2011) An investigation of the response of fish larvae to decadal changes in environmental forcing factors off the Oregon coast. Fish Oceanogr 20:314–328

Bi H, Peterson WT, Strub PT (2011) Transport and coastal zooplankton communities in the northern California Current system. Geophys Res Lett 38:L12607, doi:10.1029/2011GL047927

Bolin R, Abbott D (1963) Studies on the marine climate and phytoplankton of the central coastal area of California, 1954–1960. Calif Coop Ocean Fish Invest Rep 9:23–45

Checkley DM, Barth JA (2009) Patterns and processes in the California Current System. Prog Oceanogr 83:49–64

Clarke KR, Gorley RN (2006) PRIMER v6: user manual/tutorial. PRIMER-E, Plymouth

Du X, Peterson W (2014) Seasonal cycle of phytoplankton community composition in the coastal upwelling system off central Oregon in 2009. Estuaries Coasts 37:299–311

Frame ER, Lessard EJ (2009) Does the Columbia River plume influence phytoplankton community structure along the Washington and Oregon coasts? J Geophys Res 114:C00B09, doi:10.1029/2008JC004999

Francis TB, Scheuerell MD, Brodeur RD, Levin PS, Ruzicka JJ, Tolimieri N, Peterson WT (2012) Climate shifts the interaction web of a marine plankton community. Glob Change Biol 18:2498–2508

Garrison DL (1979) Monterey Bay phytoplankton I. Seasonal cycles of phytoplankton assemblages. J Plankton Res 1: 241–265

Henson SA, Thomas AC (2007) Phytoplankton scales of variability in the California Current System: 1. Interannual and cross-shelf variability. J Geophys Res 112:C07017, doi:10.1029/2006JC004039

Hooff RC, Peterson WT (2006) Recent increases in copepod biodiversity as an indicator of changes in ocean and climate conditions of the northern California current ecosystem. Limnol Oceanogr 51:2607–2620

Horner RA (2002) A taxonomic guide to some common marine phytoplankton. Biopress, Bristol

Jester R, Lefebvre K, Langlois G, Vigilant V, Baugh K, Silver MW (2009) A shift in the dominant toxin-producing algal species in central California alters phycotoxins in food webs. Harmful Algae 8:291–298

Kahru M, Kudela RM, Manzano-Sarabia M, Greg Mitchell B (2012) Trends in the surface chlorophyll of the California Current: merging data from multiple ocean color satellites. Deep-Sea Res II 77-80:89–98

Keister JE, Di Lorenzo E, Morgan CA, Combes V, Peterson WT (2011) Zooplankton species composition is linked to ocean transport in the Northern California Current. Glob Change Biol 17:2498–2511

Lassiter AM, Wilkerson FP, Dugdale RC, Hogue VE (2006) Phytoplankton assemblages in the CoOP-WEST coastal upwelling area. Deep-Sea Res II 53:3063–3077

Mantua NJ, Hare SR (2002) The Pacific Decadal Oscillation. J Oceanogr 58:35–44

Margalef R (1978) Life-forms of phytoplankton as survival alternatives in an unstable environment. Oceanol Acta 134:493–509

Martinez E, Antoine D, D'Ortenzio F, Gentili B (2009) Climate-driven basin-scale decadal oscillations of oceanic phytoplankton. Science 326:1253–1256

Mitchell-Innes BA, Walker DR (1991) Short-term variability during an anchor station study in the southern Benguela upwelling system: phytoplankton production and biomass in relation to species changes. Prog Oceanogr 28:65–89

Peterson WT (2009) Copepod species richness as an indicator of long-term changes in the coastal ecosystem of the northern California Current. Calif Coop Ocean Fish Invest Rep 50:73–81

Peterson WT, Schwing FB (2003) A new climate regime in northeast Pacific ecosystems. Geophys Res Lett 30:1896, doi:10.1029/2003GL017528

Peterson WT, Keister JE, Feinberg LR (2002) The effects of the 1997-99 El Niño/La Niña events on hydrography and zooplankton off the central Oregon coast. Prog Oceanogr 54:381–398

Pitcher GC, Walker DR, Mitchell-Innes BA, Moloney CL (1991) Short-term variability during an anchor station study in the southern Benguela upwelling system: phytoplankton dynamics. Prog Oceanogr 28:39–64

Siegel DA, Behrenfeld MJ, Maritorena S, McClain CR and others (2013) Regional to global assessments of phytoplankton dynamics from the SeaWiFS mission. Remote Sens Environ 135:77–91

Smayda TJ, Reynolds CS (2001) Community assembly in marine phytoplankton: application of recent models to harmful dinoflagellate blooms. J Plankton Res 23: 447–461

Smayda TJ, Trainer VL (2010) Dinoflagellate blooms in upwelling systems: seeding, variability, and contrasts with diatom bloom behaviour. Prog Oceanogr 85: 92–107

Strickland JDH, Parsons TR (1972) A practical handbook of seawater analysis, 2nd edn. Fisheries Research Board of Canada, Ottawa

Thomas AC, Brickley P, Weatherbee R (2009) Interannual variability in chlorophyll concentrations in the Humboldt and California Current Systems. Prog Oceanogr 83: 386–392

Thomas AC, Strub PT, Weatherbee RA, James C (2012) Satellite views of Pacific chlorophyll variability: comparisons to physical variability, local versus nonlocal influences and links to climate indices. Deep-Sea Res II 77–80:99–116

Tont SA (1987) Variability of diatom species populations: from days to years. J Mar Res 45:985–1006

Tweddle JF, Strutton PG, Foley DG, Higgins L and others (2010) Relationships among upwelling, phytoplankton blooms, and phycotoxins in coastal Oregon shellfish. Mar Ecol Prog Ser 405:131–145

Venrick EL (2012) Phytoplankton in the California Current system off southern California: changes in a changing environment. Prog Oceanogr 104:46–58

Wilkerson FP, Dugdale RC (1987) The use of large shipboard barrels and drifters to study the effects of coastal upwelling on phytoplankton dynamics. Limnol Oceanogr 32:368–382

Yokomizo H, Botsford L, Holland M, Lawrence C, Hastings A (2010) Optimal wind patterns for biological production in shelf ecosystems driven by coastal upwelling. Theor Ecol 3:53–63

Yoo SJ, Batchelder HP, Peterson WT, Sydemann WJ (2008) Seasonal, interannual and event scale variation in North Pacific ecosystems. Prog Oceanogr 77:155–181n

Editorial responsibility: Edward Durbin, Narragansett, Rhode Island, USA

Submitted: July 7, 2014; Accepted: October 23, 2014
Proofs received from author(s): December 20, 2014